Supplementary Material

The pulmonary endothelial glycocalyx regulates neutrophil adhesion and lung injury during experimental sepsis.

Eric P. Schmidt[1,2], Yimu Yang[1], William J. Janssen[3], Aneta Gandjeva[1], Mario J. Perez[1], Lea Barthel[3], Rachel L. Zemans[3], Joel C. Bowman[1], Dan E. Koyanagi[1], Zulma X. Yunt[3], Lynelle P. Smith[1], Sara S. Cheng[4], Katherine H. Overdier[2], Kathy R. Thompson[2], Mark W. Geraci[1], Ivor S. Douglas[1,2], David B. Pearse[5], Rubin M. Tuder[1]

[1]Program in Translational Lung Research, Division of Pulmonary Sciences and Critical Care Medicine, Department of Medicine, University of Colorado School of Medicine, Aurora, Colorado, USA. [2]Denver Health Medical Center, Denver, Colorado, USA. [3]Department of Medicine, National Jewish Health, Denver, Colorado, USA. [4]Department of Anesthesiology, University of Colorado School of Medicine, Aurora, Colorado, USA, [5]Division of Pulmonary and Critical Care Medicine, Department of Medicine, Johns Hopkins University School of Medicine, Baltimore, Maryland, USA.

Correspondence should be addressed to E.P.S. (eric.schmidt@ucdenver.edu).

Nature Medicine doi:10.1038/nm.2843

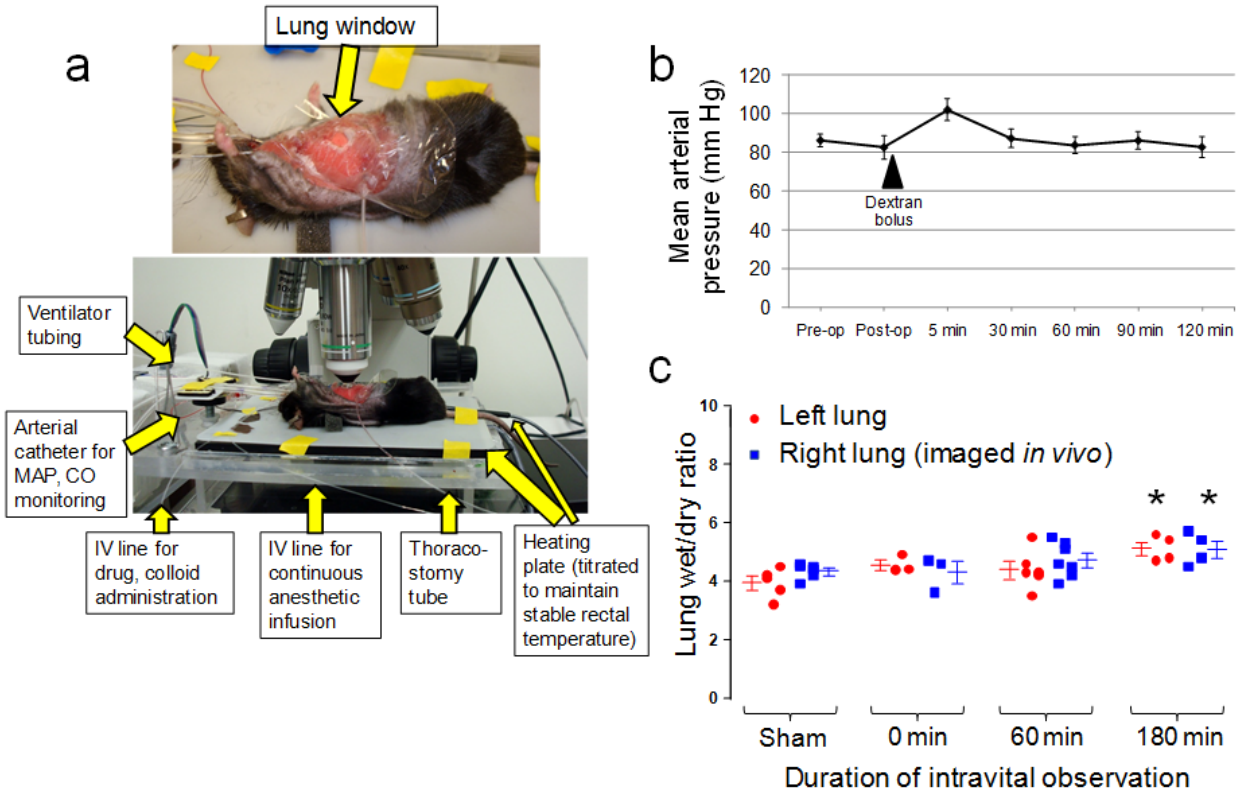

Supplementary Figure 1: Intravital mouse lung microscopy model. (**a**) Schematic of closed-chest intravital microscopy (*in vivo* microscopy, IVM) model. After placement of the right thoracic window and re-expansion of the right lung, the mouse is transitioned to the IVM stage, where ventilation, heating, sedation, and hemodynamic monitoring are continuously performed. MAP = mean arterial pressure; CO = cardiac output. (**b**) Mouse mean arterial pressure remains stable throughout the period of intravital observation. *n* = 8 mice; arrowhead represents 500 µL intravenous 6% dextran bolus. (**c**) IVM does not cause lung injury, as evidenced by stable lung wet-dry ratios throughout 60 min of observation. By 180 min of observation, an increase in wet-dry ratio is noted; however, this increased lung water occurs similarly in visualized (right) and non-visualized (left) lungs, further demonstrating that the right-sided surgical preparation does not cause lung injury. *n* = 7 – 8 wild-type mice per group; * $P < 0.05$ as compared to other time points; no significant difference exists between right and left lungs at any time point.

Nature Medicine doi:10.1038/nm.2843

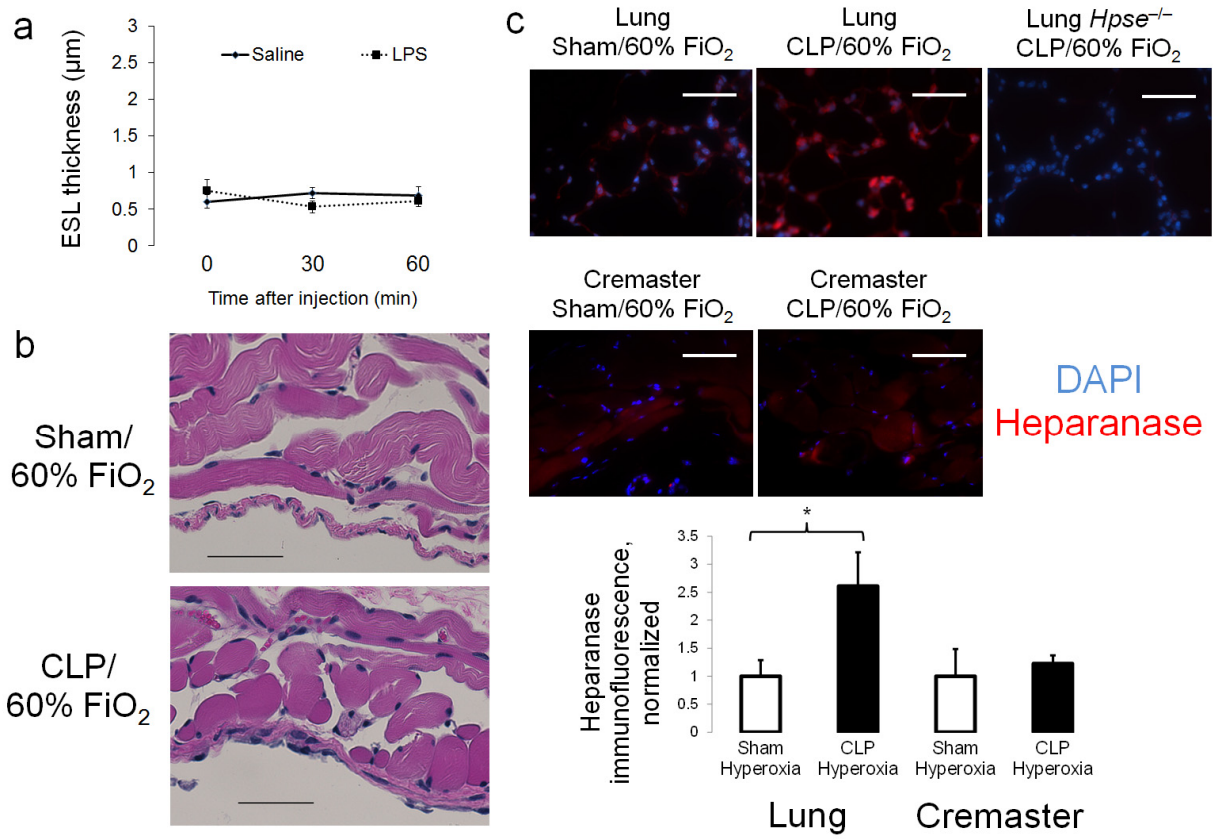

Supplementary Figure 2: Cremasteric microvasculature during endotoxemia and sepsis. (**a**) Endothelial surface layer (ESL) thickness in cremasteric microvessels (< 20 μm diameter) remains stable after intravenous saline (200 μl) or LPS (20 μg g^{-1} in 200 μl saline). Y-axis scale is identical to that used in Figures 1 and 2 of the main manuscript, highlighting differences between pulmonary and cremasteric ESL thickness. *n* = 4 – 5 mice per group. (**b**) 48 h after cecal ligation and puncture (CLP)/60% fraction inspired oxygen (FiO_2), the cremaster muscle shows no evidence of inflammation on hematoxylin and eosin staining. Images representative of 3 – 4 mice per group. (**c**) 48 h after CLP/hyperoxia, heparanase immunofluorescence is increased in lungs but not in the cremaster muscle. No heparanase immunofluorescence is noted in *Hpse*$^{-/-}$ mice. DAPI = nuclear stain. * *P* < 0.05. *n* = 3 – 6 mice per group. Bar represents 50 μm in (b, c).

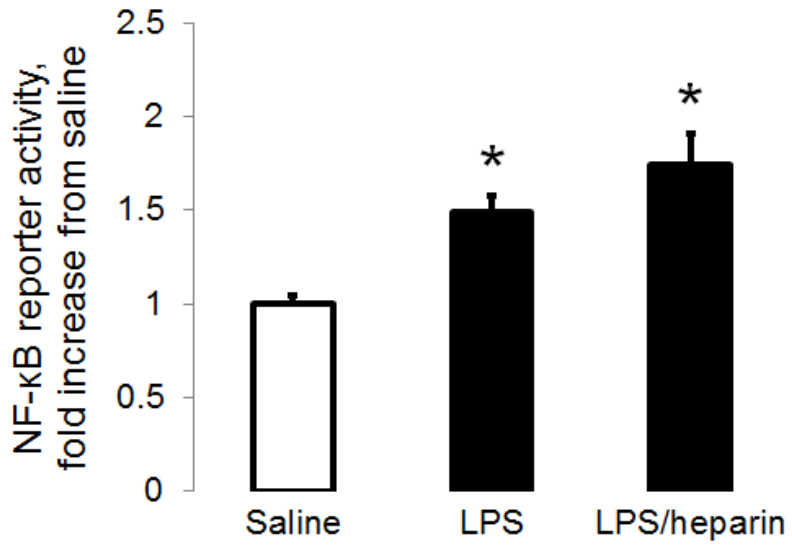

Supplementary Figure 3: Heparin does not interfere with LPS danger signaling. LPS activation of MLE-15 cells was measured via NFκB-dependent reporter *Firefly* luciferase activity after treatment with saline, LPS (1 μg ml^{-1}), or LPS plus heparin (0.4 units ml^{-1}, consistent with therapeutic plasma levels[1]) for 4 h. The presence of heparin does not impede LPS signaling, consistent with previous studies[2] as well as the observed (Supplementary Figure 9a) lack of heparin interference with LPS induction of ICAM-1, a NFκB-regulated adhesion molecule[3]. Data normalized to *Renilla* luciferase activity; $n = 3$ experiments per group; * $P < 0.05$ in comparison to saline.

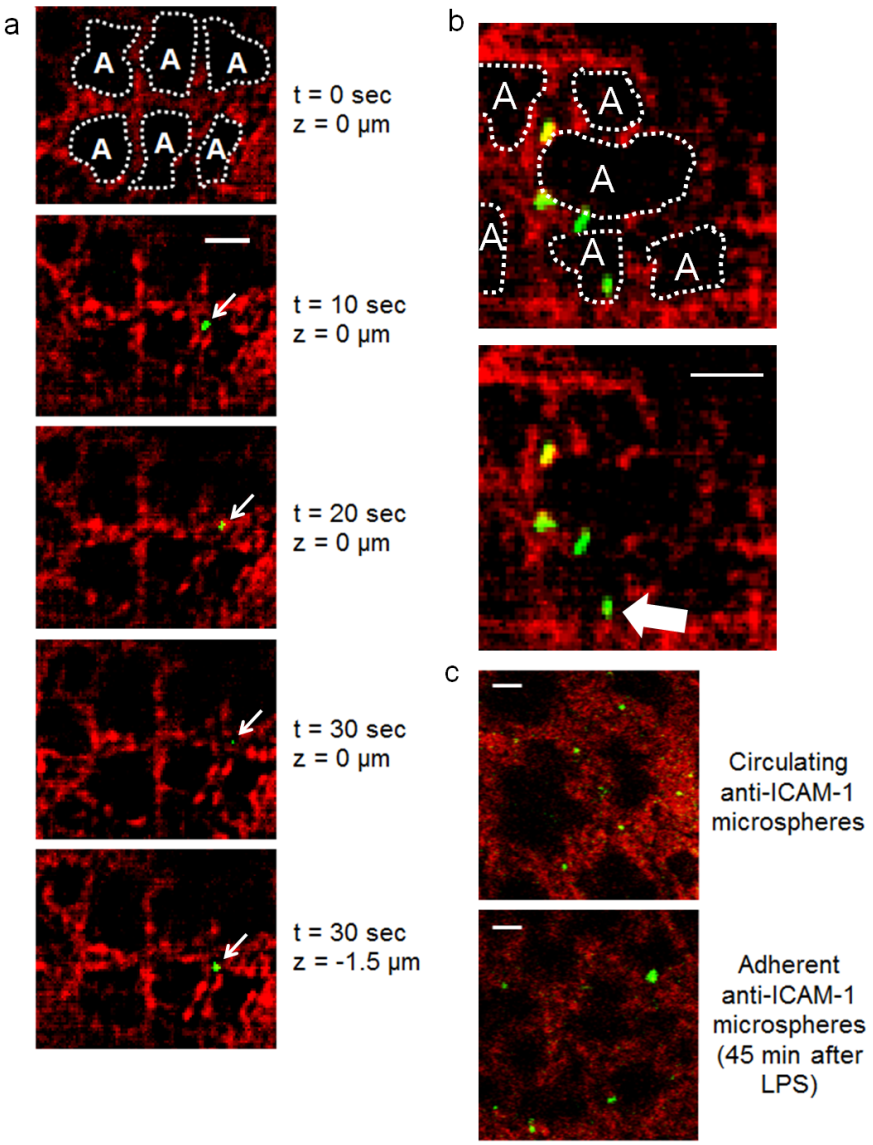

Supplementary Figure 4: The intact ESL excludes circulating neutrophils and microspheres. (**a**,**b**) GFP^+ neutrophils (green) injected into wild-type mice pass through the pulmonary microcirculation. Using high-speed confocal IVM, a single neutrophil (arrow) is visualized moving through an interalveolar microvessel, then turning to enter a microvessel penetrating proximally into the lung (**a**). During this transit, the neutrophil remains within a 150 kDa TRITC-dextran column (red, excluded by the ESL), suggesting that circulating, unstimulated neutrophils tend to be excluded by the ESL. 45 min after intravenous LPS (20 µg g^{-1}), adherent neutrophils surround alveoli (**b**). Adherent neutrophils are stationary at the periphery of the TRITC-dextran column, consistent with the loss of an ESL that excludes both neutrophils and TRITC-dextran. Arrow: extravasated neutrophil within the alveolus. (**c**) Fluorescent anti-ICAM-1 microspheres (green) demonstrate similar behavior as neutrophils before and after intravenous LPS (20 µg g^{-1}). Even with high-speed confocal imaging, resolution of closed-chest mouse IVM is insufficient to determine neutrophil or microsphere interactions with the post-LPS remnant (< 0.5 µm) glycocalyx. Images in (a – c) representative of 3 separate experiments. Bar = 20 µm. A = alveolus.

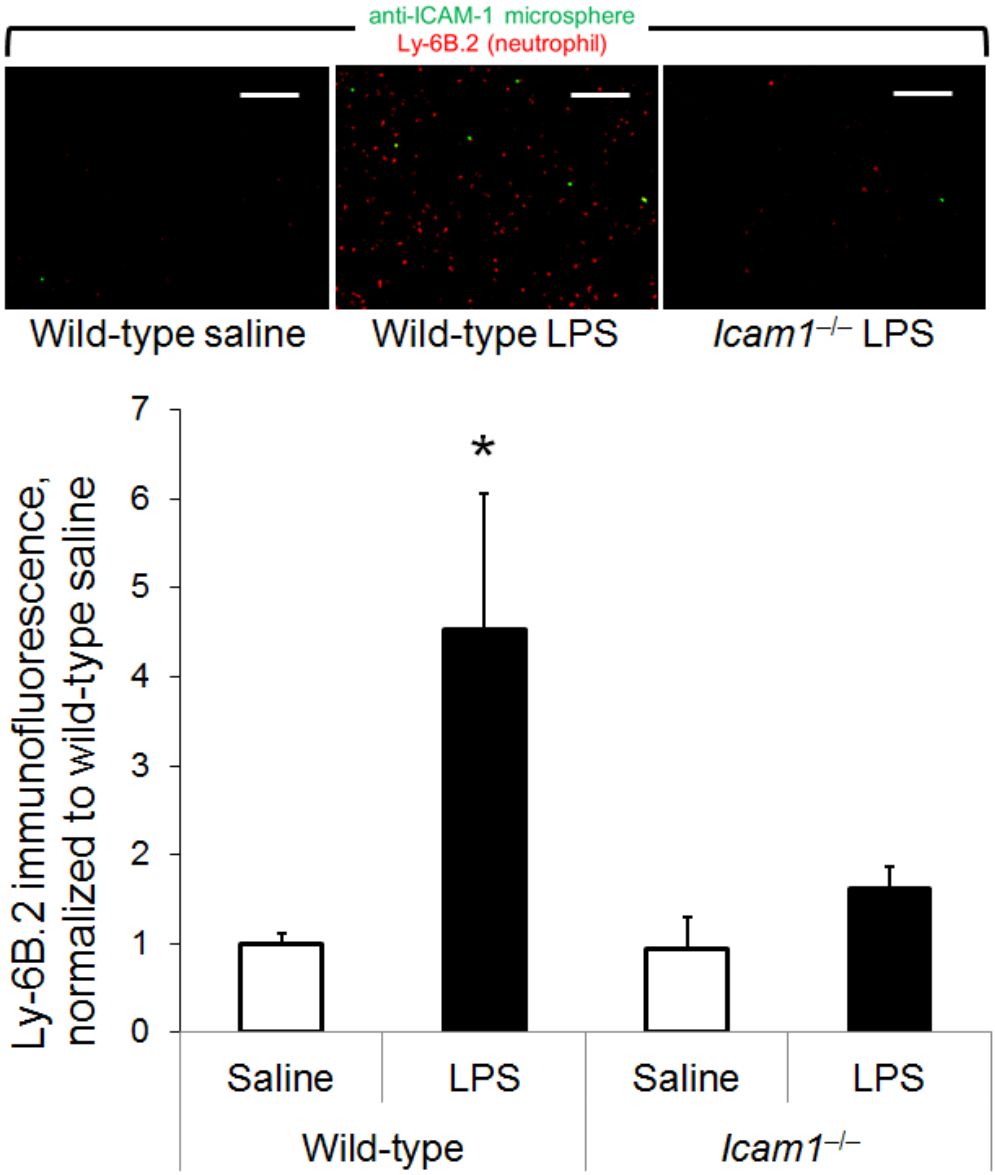

Supplementary Fig 5: ICAM-1 participates in pulmonary neutrophil adhesion 45 min after intravenous LPS. Intravenous LPS treatment (20 μg g^{-1}, 45 min) induces pulmonary neutrophil adhesion in wild-type mice, as measured via Ly-6B.2 immunofluorescence of frozen sections of non-IVM imaged mouse lungs. LPS-induced neutrophil adhesion is attenuated in ICAM-1 knock-out (*Icam1*$^{-/-}$) mice. These findings are consistent with previous reports demonstrating the importance of ICAM-1 to endotoxin-induced lung injury (reference 17 of main manuscript). Importantly, attenuation of LPS-induced neutrophil adhesion is not complete in *Icam1*$^{-/-}$ mice (P = 0.06 comparing wild-type LPS to *Icam1*$^{-/-}$ LPS by t-test), demonstrating potential relevance of other endothelial surface molecules (such as VCAM-1) to the processes of neutrophil adhesion and extravasation during endotoxemia. * $P < 0.05$ in comparison to wild-type saline; n = 3 – 4 mice per group. Bar = 50 μm.

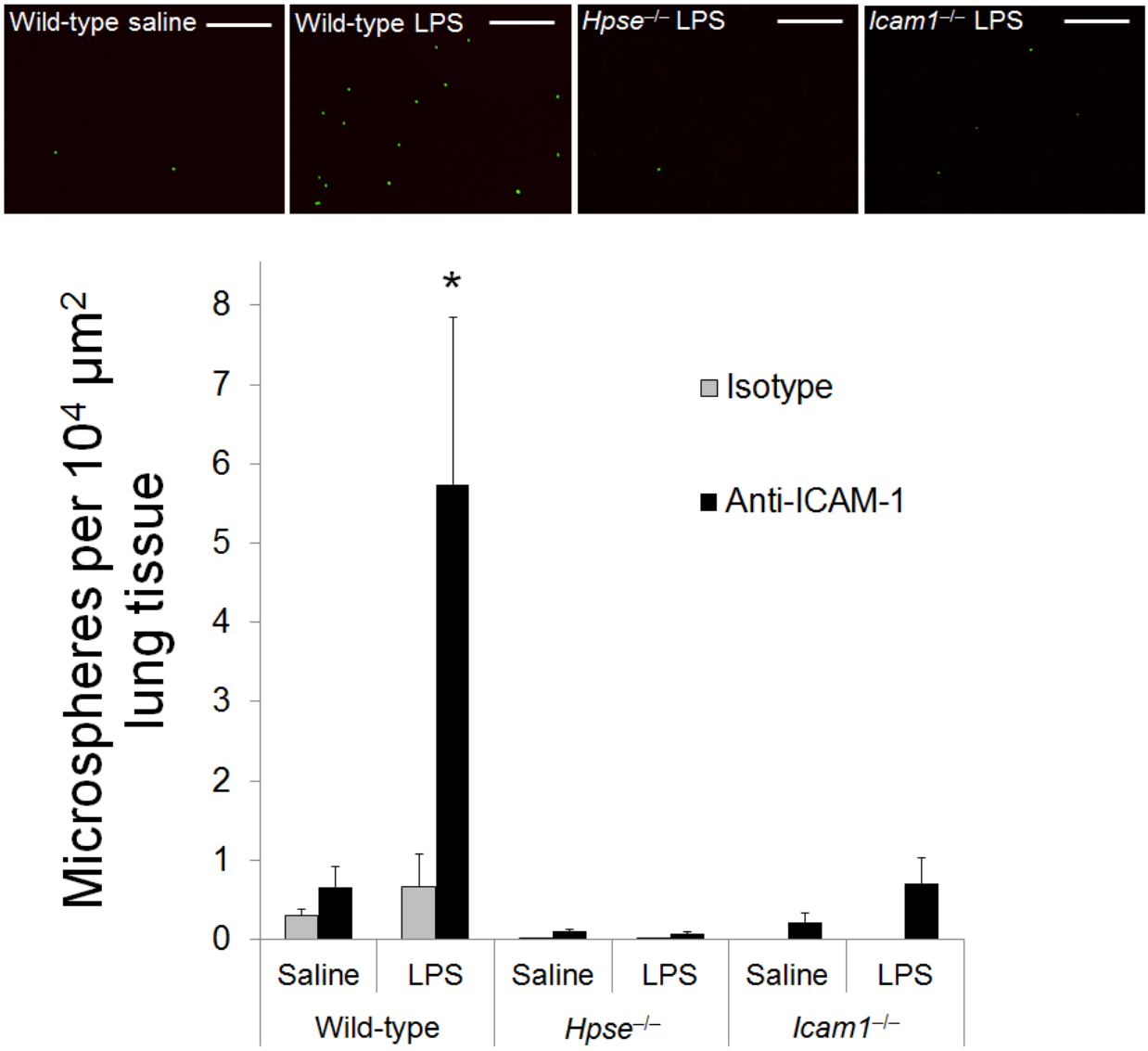

Supplementary Figure 6: Anti-ICAM-1 microsphere adhesion observed via IVM similarly occurs within the contralateral mouse lung. Frozen sections of left lungs (not imaged during mouse IVM) reveal increased anti-ICAM-1 microsphere adhesion 45 min after intravenous LPS (20 µg g^{-1}), consistent with findings obtained via intravital imaging of right lungs (Figure 3b). LPS induction of microsphere adhesion does not occur in heparanase knock-out (*Hpse*$^{-/-}$) mice, consistent with the ability of the intact glycocalyx to limit access to endothelial surface adhesion molecules. Isotype-matched antibody-coated microspheres and *Icam1*$^{-/-}$ mice serve as negative controls (isotype microsphere experiments were not performed on *Icam1*$^{-/-}$ mice). Counts performed on 10 random low-powered fields per mouse. n = 3 – 5 mice per group. * P < 0.05 in comparison to wild-type saline anti-ICAM-1 control. Bar = 50 µm. No microsphere adhesion was noted during intravital imaging of the right lungs of *Icam1*$^{-/-}$ mice (n = 3, data not shown).

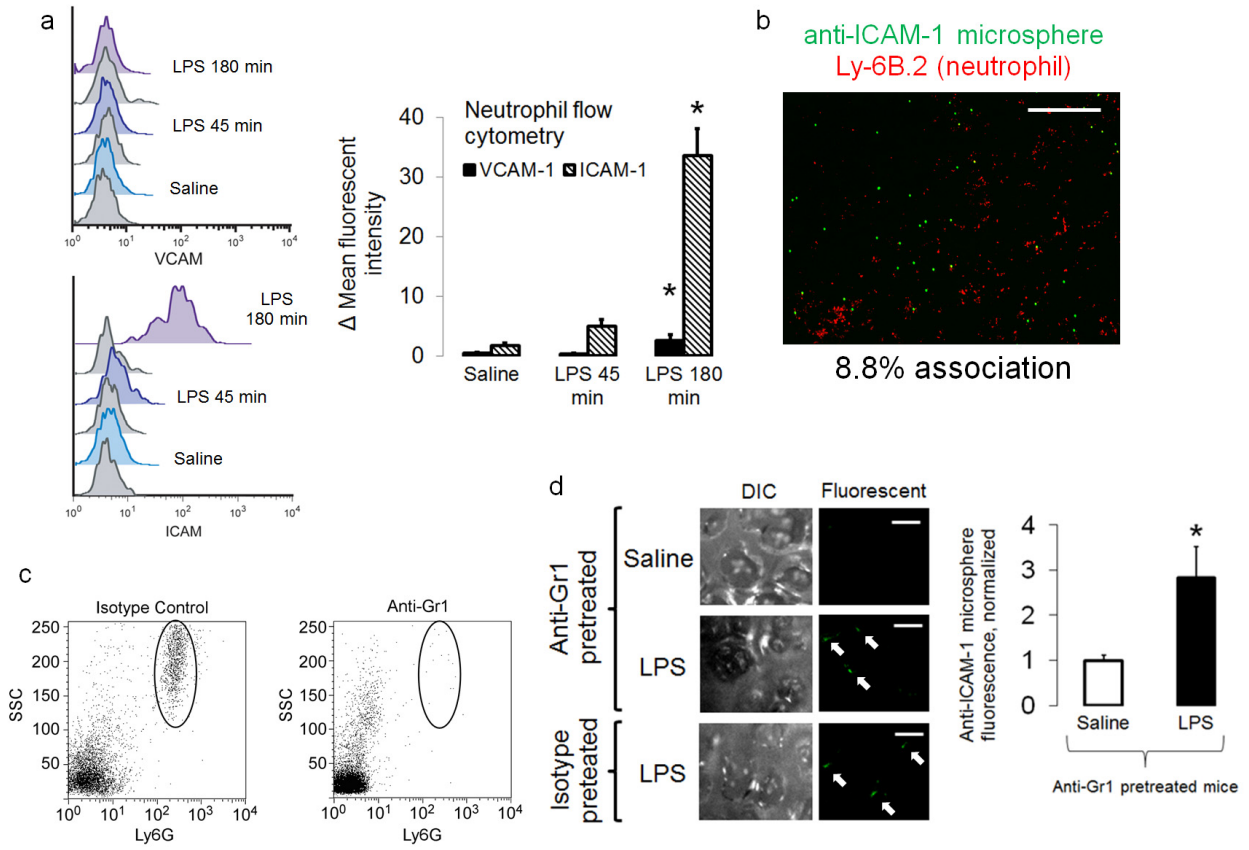

Supplementary Figure 7: Neutrophils are not the target of microsphere binding. Activated neutrophils may express ICAM-1[4]. However, anti-ICAM-1 microsphere adhesion observed within the pulmonary microcirculation 45 min after 20 μg g^{-1} intravenous LPS (Fig 3b) is not due to neutrophil binding, as (**a**) 45 min LPS exposure is insufficient to increase neutrophil ICAM-1 expression, as determined by flow cytometry of peripheral blood neutrophils. Accordingly, anti-VCAM-1 microsphere adhesion within the pulmonary microcirculation observed 45 min after LPS (20 μg g^{-1}, Supplementary Figure 8a) is not due to neutrophil binding, as no induction of neutrophil VCAM-1 occurs. In contrast, significant induction of neutrophil ICAM-1 and VCAM-1 occurs 180 min after intravenous LPS (20 μg g^{-1}). Staggered histograms indicate fluorescent intensity (colored: anti-ICAM-1 or anti-VCAM-1; grey: isotype control) of representative experiments. Δ mean fluorescent intensity represents difference in fluorescence from isotype controls. n = 6 – 9 mice per group; * $P < 0.05$ from saline. (**b**) Lung frozen sections from anti-ICAM-1 microsphere-injected, 45 min LPS (20 μg g^{-1})-treated mice demonstrate minimal microsphere-neutrophil association, likely reflecting random approximation to a common target. Quantification reflects images from 4 LPS-treated mice. Bar = 200 μm. (**c**,**d**) Pretreatment with anti-Gr1 antibody (125 μg i.p. 48 h and 24 h prior to microscopy) depletes peripheral neutrophils ($Ly6G^+$, SSC-hi); no depletion occurs in isotype-treated mice (**c**). Neutrophil depletion does not prevent anti-ICAM-1 microsphere adhesion (arrows) 45 min after intravenous LPS (20 μg g^{-1}) as demonstrated by IVM (**d**). n = 3 mice per group (n = 2 for isotype-pretreated). * $P < 0.05$. Bar = 20 μm.

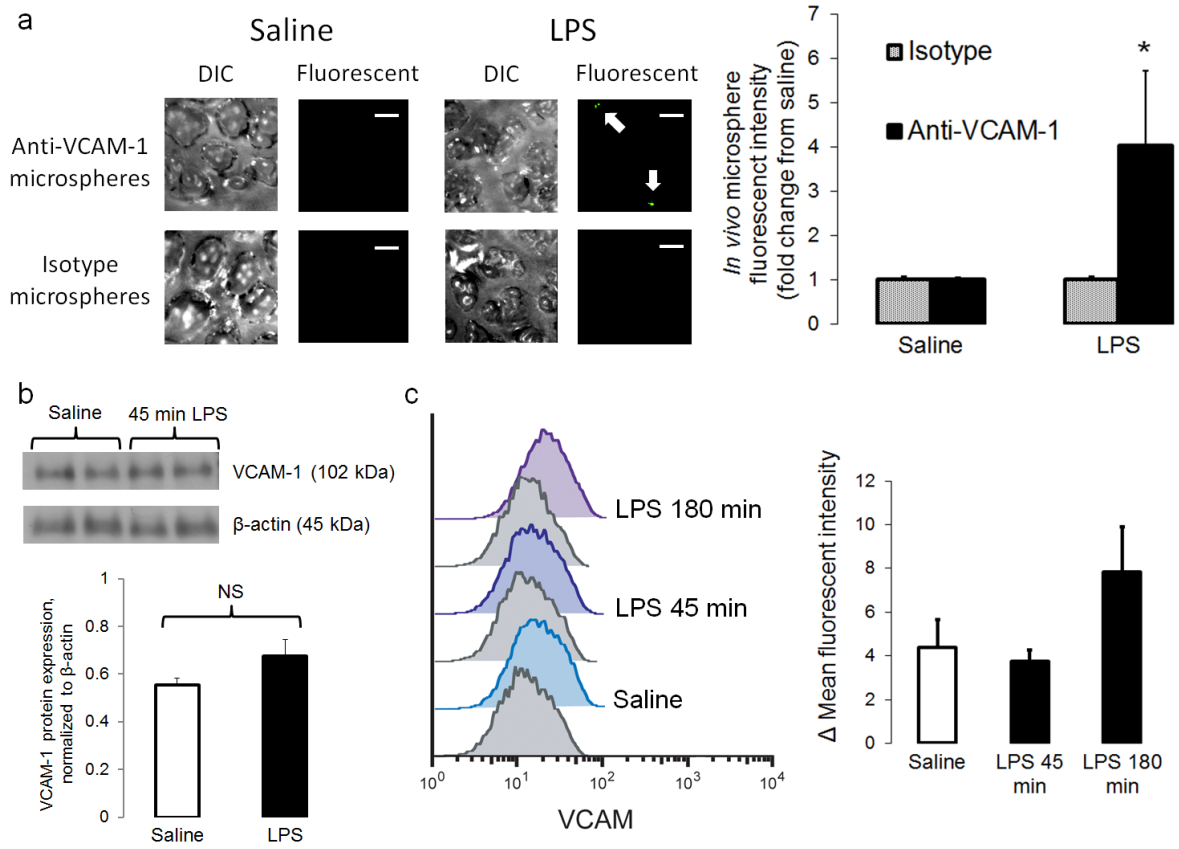

Supplementary Figure 8: Short-duration LPS treatment increases exposure of pulmonary microvascular VCAM-1 to circulating microspheres. (**a**) Visualization of anti-VCAM-1 coated fluorescent microspheres within wild-type mouse subpleural microvessels, simultaneously imaged by differential interference contrast (DIC) and fluorescence IVM. Images obtained 45 min after intravenous saline or LPS (20 μg g^{-1}). While infrequent (consistent with relatively low levels of constitutive VCAM-1 expression[5]), microsphere adhesion is consistently and exclusively noted in LPS-treated mice (arrows). Isotype-matched antibody-coated microspheres serve as controls for nonspecific adhesion. Bar = 20 μm. *n* = 3 mice per group; * *P* < 0.05 from saline. (**b**,**c**) Increased VCAM-1 availability 45 min after LPS is not due to increased cell-surface expression, as demonstrated by (**b**) stable total VCAM-1 in mouse lung microvascular endothelial cells 45 min after saline (vehicle) or LPS (10 μg ml^{-1}, *n* = 4 per group) and (**c**) stable cell-surface VCAM-1 on flow cytometry of endothelial cells ($CD45^{-}$, $CD31^{+}$, $CD141^{+}$) identified in mouse lung digestates. Lungs undergoing digestion were harvested 45 min after intravenous saline (200 μl) or 45 or 180 min after intravenous LPS (20 μg g^{-1} in 200 μl saline). Staggered histograms indicate fluorescent intensity (colored: anti-VCAM-1; grey: isotype control) of representative experiments. Δ mean fluorescent intensity represents difference in fluorescence from isotype controls; *n* = 5 – 6 mice per group. Flow cytometry confirms low levels of constitutive VCAM-1 expression (in contrast to ICAM-1, Supplementary Fig 9d), consistent with infrequency of observed microsphere adhesion.

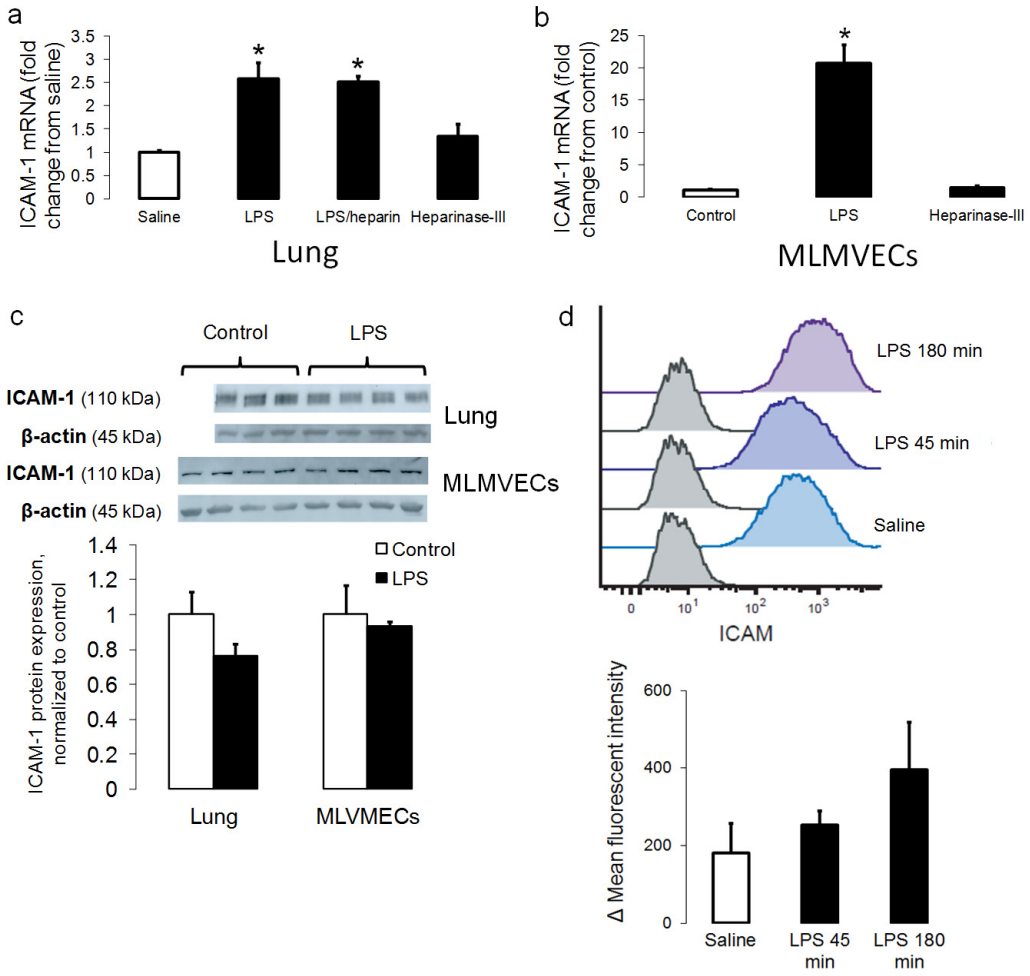

Supplementary Figure 9 : Short-duration LPS exposure does not increase ICAM-1 protein expression. (**a**) Relative expression of ICAM-1 mRNA in lungs of wild-type mice 45 min after treatment with intravenous saline, LPS (20 μg g^{-1}), LPS (20 μg g^{-1}) with heparin (5 units), or heparinase-III (1 unit). Normalized to cyclophilin A mRNA; *n* = 3 – 4 per group; * *P* < 0.05 from saline. (**b**) Relative expression of ICAM-1 mRNA in cultured mouse lung microvascular endothelial cells (MLMVECs) treated with diluent, LPS (10 μg ml^{-1}) or heparanase-III (50 mU ml^{-1}) for 45 min. Normalized to cyclophilin A mRNA; *n* = 4 per group; * *P* < 0.05 from control. (**c**) ICAM-1 protein expression in MLMVECs or lungs of wild-type mice 45 min after treatment with diluent or LPS, as described in (a,b). Expression normalized to β-actin. (**d**) Flow cytometry of endothelial cells ($CD45^-$, $CD31^+$, $CD141^+$) identified in mouse lung digestates. Lungs undergoing digestion (a process that removes the glycocalyx, as detailed in the Online Methods) were harvested 45 min after intravenous saline (200 μl) or 45 or 180 min after intravenous LPS (20 μg g^{-1} in 200 μl saline). Staggered histograms indicate fluorescent intensity (colored: anti-ICAM-1; grey: isotype control) of representative experiments. Δ mean fluorescent intensity represents difference in fluorescence from isotype controls; *n* = 5 – 6 mice per group.

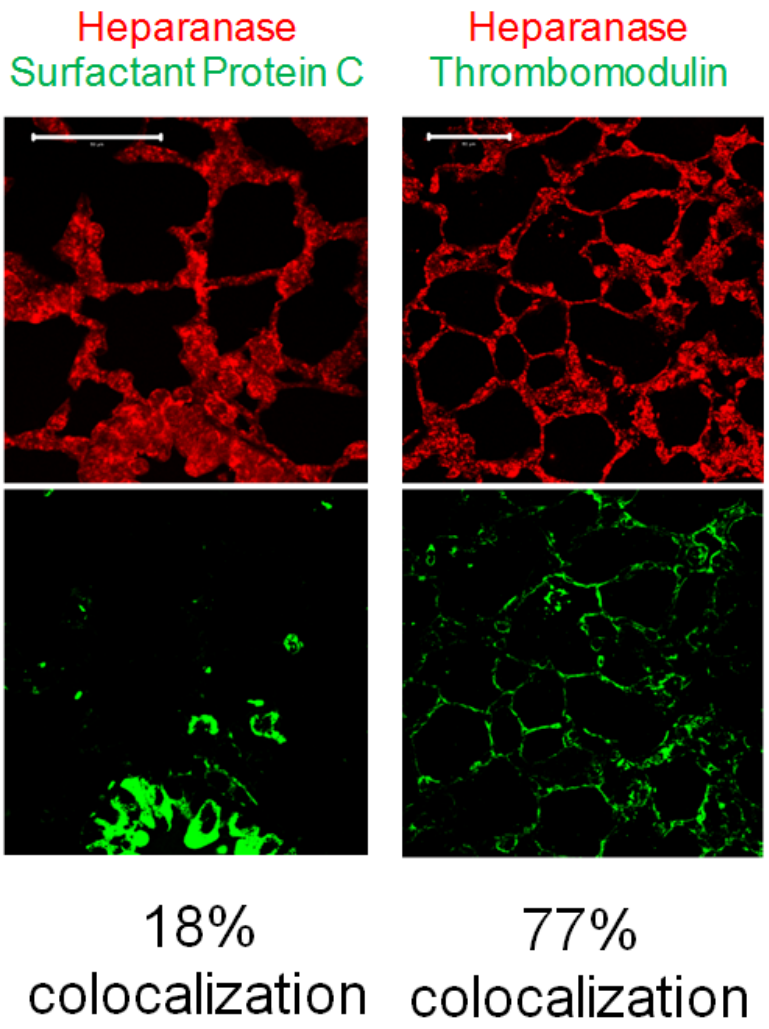

Supplementary Figure 10: Heparanase colocalization with epithelium, endothelium. Confocal images of wild-type mouse lungs harvested 6 h after intraperitoneal LPS (40 μg g^{-1}). Left: minimal colocalization is noted between heparanase (red) and surfactant protein C (type II epithelial cell marker, green). Right: Significant colocalization exists between heparanase and thrombomodulin (endothelial cell marker, green), consistent with quantification of widefield fluorescent images in Figure 4d of the main manuscript. Representative of 3 wild-type mice per group; isotype controls showed no fluorescence (not shown). Bar = 50 μm.

Nature Medicine doi:10.1038/nm.2843

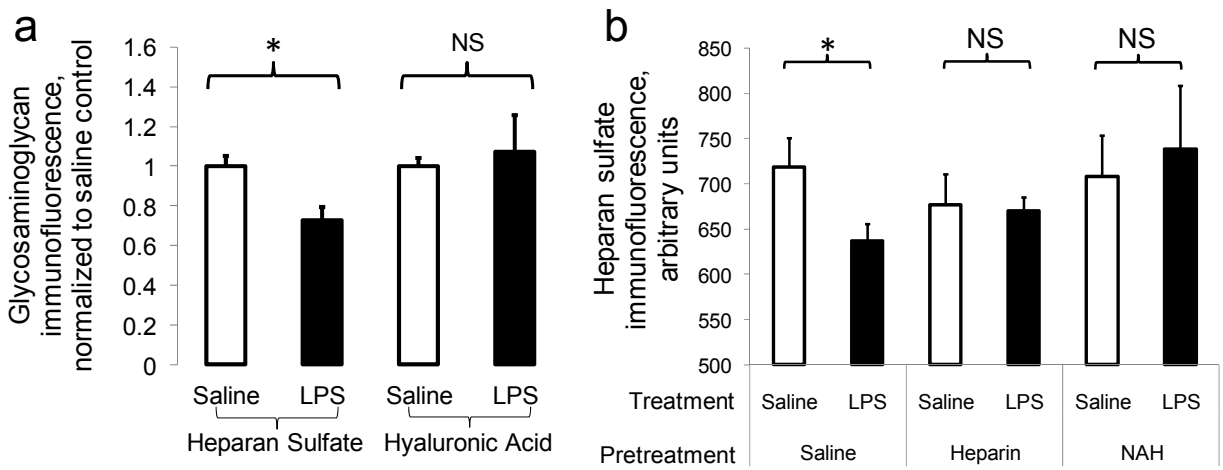

Supplementary Figure 11: LPS-induced glycocalyx degradation is specific to heparan sulfate. (**a**) Assessment by immunofluorescence of glycosaminoglycan expression within pulmonary vessels of wild-type mice 6 h after intraperitoneal LPS (40 μg g^{-1}) or saline. Heparan sulfate content is decreased along the surface of small (< 100 μm) perfusion-fixed pulmonary vessels, while hyaluronic acid content is spared, demonstrating a heparan sulfate-specific mechanism of glycocalyx degradation. n = 6 – 7 mice per group, > 5 vessels per mouse; * P < 0.05. (**b**) Assessment by immunofluorescence of heparan sulfate expression in small pulmonary vessels of wild-type mice 6 h after intraperitoneal LPS (40 μg g^{-1}) or saline following a 3 hour pretreatment with subcutaneous saline, heparin (5 units), or N-desulfated/ReN-acetylated heparin (NAH, 150 μg). Heparanase inhibition prevents loss of vascular heparan sulfate content, suggesting that heparanase mediates the specific loss of glycocalyx heparan sulfate during endotoxemia. n = 4 – 8 mice per group; > 5 vessels per mouse; * P < 0.05.

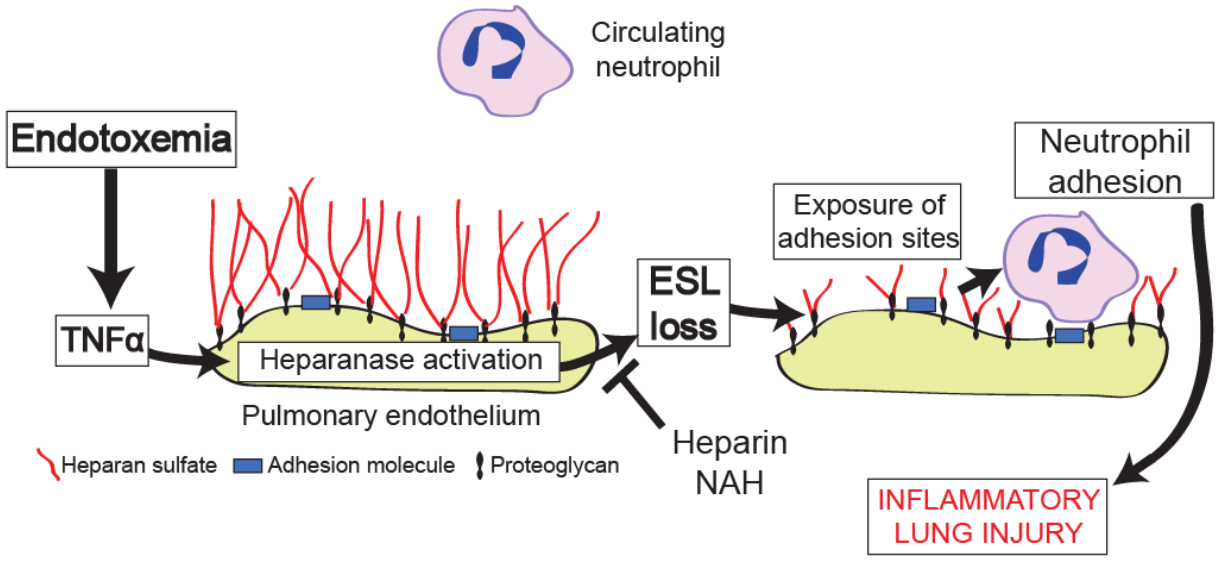

Supplementary Figure 12: Proposed paradigm for heparanase-ESL signaling in sepsis-associated acute lung injury. During health, the pulmonary microvascular ESL is substantial and excludes circulating neutrophils. During endotoxemia, endothelial heparanase is activated via post-translational modification (cleavage), followed by an increase in expression. Active heparanase degrades glycocalyx heparan sulfate, leading to loss of ESL thickness. While this loss of ESL thickness is not complete (i.e. a remnant < 0.5 μm ESL remains), degradation is sufficient to induce exposure of endothelial surface adhesion molecules with consequent neutrophil adhesion. Heparanase inhibition by coagulant or nonanticoagulant (NAH) heparins may therefore prevent the onset of sepsis-associated inflammatory lung injury.

Nature Medicine doi:10.1038/nm.2843

	Healthy Donors	Acute Respiratory Failure				
		Altered Mental Status	Pneumonia	Non-pulmonary sepsis	All patients	*P* value
Number of subjects	4	4	7	4	15	
Age (years)		62 ± 2.34	48.14 ± 4.65	56.25 ± 1.93	54 ± 2.70	0.09
Sex (male)	50%	50%	29%	75%	46.6%	0.38
Ethnicity (Caucasian)		25%	57%	50%	46.6%	0.63
Current smokers		50%	57%	50%	53.3%	0.97
Time from intubation to blood draw (h)		41.38 ± 4.8	34.11 ± 7.06	35.44 ± 7.52	36.39 ± 3.90	0.76
APACHE II score at blood draw		24.25 ± 3.47	20.14 ± 1.5	21.25 ± 6.24	21.53 ± 1.89	0.7
ICU LOS (days)		5.58 ± 2.41	11.88 ± 3.04	13.39 ± 3.19	10.71 ± 1.84	0.29
Hospital mortality		50%	29%	0%	26.7%	0.32

Supplementary Table 1. Demographic and clinical information from healthy plasma donors (left) and critically-ill patients undergoing mechanical ventilation for acute respiratory failure (Fig 5a). Where appropriate, ± S.E.M. reported. *P* value represents ANOVA of characteristics across 3 groups with acute respiratory failure. APACHE II: "Acute Physiology and Chronic Health Evaluation II"; higher scores indicate more severe disease. LOS: length of stay.

Patient demographics	**Clinical History**	**Pathologic diagnosis** (from surgical lung biopsy)	**Lung heparanase immunofluorescence** (fold increase from mean fluorescence in normal lungs, *n* = 3)
82 y/o male	Idiopathic acute interstitial pneumonitis.	Diffuse alveolar damage with organization and giant cells	8.27 (**Fig 5c**)
63 y/o female	Remote history of solid organ transplantation. Septic shock and respiratory failure.	Acute and organizing diffuse alveolar damage	6.87
44 y/o male	Remote history of solid organ transplantation. Sepsis and respiratory failure.	Diffuse alveolar damage with focal organizing pneumonia	5.15
48 y/o male	Chemotherapy-induced respiratory failure.	Acute lung injury	1.78
55 y/o female	Acute exacerbation of interstitial lung disease.	Acute lung injury with diffuse alveolar damage and focal organizing pneumonia	10.06
45 y/o female	Amiodarone-associated acute respiratory failure.	Diffuse alveolar damage, organizing phase	4.73
57 y/o male	Recent organ transplantation. Septic shock with acute respiratory failure.	Acute and organizing diffuse alveolar damage	6.00
61 y/o male	Remote history of solid organ transplantation. Acute respiratory failure.	Acute and organizing diffuse alveolar damage	6.76
62 y/o male	Acute exacerbation of interstitial lung disease.	Diffuse alveolar damage with focal alveolar hemorrhage, mild organizing pneumonia and focal interstitial fibrosis.	4.44
51 y/o male	Remote history of solid organ transplantation. Acute respiratory failure.	Severe diffuse alveolar damage.	25.21
40 y/o male	Unknown.	*Pneumocystis jirovecii* infection with diffuse alveolar damage.	11.57

Supplementary Table 2. Demographic, clinical, and pathologic information from patients with lung biopsies demonstrating diffuse alveolar damage (Fig 5b).

Supplementary Reference List

1. Raschke,R., Hirsh,J., & Guidry,J.R. Suboptimal monitoring and dosing of unfractionated heparin in comparative studies with low-molecular-weight heparin. *Ann. Intern. Med* **138**, 720-723 (2003).

2. Heinzelmann,M. & Bosshart,H. Heparin binds to lipopolysaccharide (LPS)-binding protein, facilitates the transfer of LPS to CD14, and enhances LPS-induced activation of peripheral blood monocytes. *J Immunol.* **174**, 2280-2287 (2005).

3. Roebuck,K.A. & Finnegan,A. Regulation of intercellular adhesion molecule-1 (CD54) gene expression. *J Leukoc. Biol.* **66**, 876-888 (1999).

4. Wang,J.H. *et al.* Intercellular adhesion molecule-1 (ICAM-1) is expressed on human neutrophils and is essential for neutrophil adherence and aggregation. *Shock* **8**, 357-361 (1997).

5. Henninger,D.D. *et al.* Cytokine-induced VCAM-1 and ICAM-1 expression in different organs of the mouse. *J Immunol* **158**, 1825-1832 (1997).